

A conserved basic loop in hepatitis C virus p7 protein is required for amantadine-sensitive ion channel activity in mammalian cells but is dispensable for localization to mitochondria

Stephen D. C. Griffin,¹ Ruth Harvey,^{3†} Dean S. Clarke,¹ Wendy S. Barclay,² Mark Harris¹ and David J. Rowlands¹

Correspondence
David J. Rowlands
D.J.Rowlands@bmb.leeds.ac.uk

¹Astbury Centre of Molecular Biology, School of Biochemistry and Microbiology, University of Leeds, Leeds LS2 9JT, UK

²School of Animal and Microbial Sciences, University of Reading, Whiteknights, PO Box 228, Reading, Berkshire RG6 6AJ, UK

³Sir William Dunn School of Pathology, University of Oxford, South Parks Road, Oxford OX1 3RE, UK

We previously identified the function of the hepatitis C virus (HCV) p7 protein as an ion channel in artificial lipid bilayers and demonstrated that this *in vitro* activity is inhibited by amantadine. Here we show that the ion channel activity of HCV p7 expressed in mammalian cells can substitute for that of influenza virus M2 in a cell-based assay. This was also the case for the p7 from the related virus, bovine viral diarrhoea virus (BVDV). Moreover, amantadine was shown to abrogate HCV p7 function in this assay at a concentration that specifically inhibits M2. Mutation of a conserved basic loop located between the two predicted *trans*-membrane alpha helices rendered HCV p7 non-functional as an ion channel. The intracellular localization of p7 was unaffected by this mutation and was found to overlap significantly with membranes associated with mitochondria. Demonstration of p7 ion channel activity in cellular membranes and its inhibition by amantadine affirm the protein as a target for future anti-viral chemotherapy.

Received 8 September 2003
Accepted 6 November 2003

INTRODUCTION

Hepatitis C virus (HCV) is now the leading indicator for liver transplant surgery in the West and, according to World Health Organization figures, currently infects over 3% of the world population. Mild or often asymptomatic acute infection leads to persistence in the majority of cases with most patients being unaware that they carry the virus. In a high proportion of patients, chronic infection eventually leads to the future onset of liver disorders such as cirrhosis or, in the worst cases, hepatocellular carcinoma: a highly aggressive tumour with a poor prognosis (Choo *et al.*, 1992). Treatment in the clinic is currently limited to anti-viral chemotherapy involving a combination of type 1 interferon and the guanosine analogue ribavirin, though this regime is expensive, poorly tolerated and ineffective against some of the more common viral genotypes. Vaccine development is hindered by the lack of good *in vitro* and *in vivo* models of infection, the antigenic heterogeneity of the virus and its ability to avoid immune defences. Consequently, the

identification of new viral drug targets is especially important in the search for control strategies for the disease.

HCV is the prototype member of the *Hepacivirus* genus of the family *Flaviviridae* (Robertson *et al.*, 1998). The virus is enveloped and has a single-stranded positive-sense RNA genome of around 9.6 kb, which is replicated in the cytosol via a negative-strand intermediate. An internal ribosome entry site (IRES) drives translation of a single polyprotein of approximately 3000 amino acids which is then proteolytically cleaved by cellular and viral proteases into the mature virus gene products: Core-E1-E2-p7-NS2-NS3-NS4A-NS4B-NS5A-NS5B (Clarke, 1997). Core, with the two viral glycoproteins E1 and E2, comprise the structural proteins of the virion. The non-structural (NS) proteins are thought to form a ribonucleoprotein complex with the virus genome that associates with intracellular membranes and is the site of RNA replication effected by the NS5B protein (Schmidt-Mende *et al.*, 2001; Egger *et al.*, 2002).

The p7 protein of HCV lies at the junction between the structural and non-structural regions of the virus polyprotein (Lin *et al.*, 1994; Mizushima *et al.*, 1994), though it is not known whether p7 is a virion component. The protein is small (63 amino acids) and highly hydrophobic

†Present address: PHLS Central Public Health Laboratory, Colindale, London NW9 5HT, UK.

Published ahead of print on 14 November 2003 as DOI 10.1099/vir.0.19634-0.

in nature, largely comprising two predicted *trans*-membrane alpha helices, and has been shown to be an integral membrane protein (Carrere-Kremer *et al.*, 2002). We previously identified the function for p7 as an oligomeric ion channel capable of mediating cation flow across artificial membranes, using p7 from the 1b genotype of HCV (Griffin *et al.*, 2003). Others have since demonstrated similar activity for a genotype 1a p7, suggesting a likely conservation of function across all HCV genotypes (Pavlovic *et al.*, 2003), though extended studies with p7s from various genotypes will be necessary to confirm this. This finding confirms that HCV p7 belongs to an expanding family of viral proteins known as viroporins, which are small hydrophobic proteins encoded by a variety of RNA viruses that oligomerize to form cation channels most often involved in virus assembly or entry/exit, though many have additional functions (Liljestrom *et al.*, 1991; Duff & Ashley, 1992; Pinto *et al.*, 1992; Aldabe & Carrasco, 1995; Loewy *et al.*, 1995; Tian *et al.*, 1995; Ewart *et al.*, 1996; Newton *et al.*, 1997; van Kuppeveld *et al.*, 1997; Gonzalez & Carrasco, 1998). The best-characterized viroporin is the M2 ion-channel of influenza A virus: the target of the antiviral drug, amantadine (Hay *et al.*, 1985). We showed that p7 ion channel activity could also be inhibited by amantadine (Griffin *et al.*, 2003), present at a concentration shown to specifically inhibit M2 *in vitro* (Duff & Ashley, 1992). Given that the p7 protein of the related pestivirus, bovine viral diarrhoea virus (BVDV), has been shown to be essential for the production of infectious virus particles (Harada *et al.*, 2000), it is likely that HCV p7 also plays an important role in the virus life-cycle.

As p7 is dispensable for RNA replication in subgenomic HCV replicons, it was necessary to use an alternative system to measure p7 ion channel activity in intact cells. Given that amantadine inhibits both M2 and p7 *in vitro*, we decided to test p7 in a cell-based assay designed to measure M2 function. We found that p7 was indeed functional in this assay and that its activity was inhibited by amantadine. In addition, the p7 of BVDV was also able to substitute for M2 in this assay, indicative of ion channel activity. As we have previously shown for HCV p7 (Griffin *et al.*, 2003), the BVDV p7 protein was able to oligomerize both *in vitro* and in cells, further strengthening the case for these proteins being functional and structural homologues.

Mutation of the conserved cytosolic loop located between the *trans*-membrane alpha helices of HCV p7 abrogated ion channel function in this system. Co-expression of this mutant with wild-type HCV p7 inhibited wild-type activity. No defect in expression was caused by the mutation and both proteins displayed a similar intracellular localization. Co-localization of p7 with fluorescent markers for cellular organelles indicated that it largely accumulated in membranes associated with mitochondria. This work is the first demonstration of p7 ion channel function in living cells and provides a method for analysing the function of p7 mutants or screening potential inhibitory compounds.

METHODS

DNA constructs. Constructs for the expression of p7 from the HCV 1b J4 infectious clone, influenza virus H5 haemagglutinin (HA) and M2 proteins have been described (Griffin *et al.*, 2003; R. M. A. Harvey, M. Zambon & W. S. Barclay, in press). Epitope tags were incorporated into specific primers used to amplify the p7 ORF by PCR using Vent polymerase (NEB) and either the J4 infectious clone of HCV (Yanagi *et al.*, 1998) or the CP7 infectious clone of BVDV-1 (Meyers *et al.*, 1996) as template. All PCR amplifiers for pCDNA3.1-based constructs – pCDNA FLAG-p7, C-E1-E2-p7FLAG, E1-E2-p7FLAG, HIS₆-p7, BVDVp7 and BVDVHIS₆p7 – were digested with *EcoRI* and *NotI* and ligated into an appropriately digested vector. For GFP fusion constructs, the same amplifiers were digested with *EcoRI* and *PstI* prior to cloning into pGFP-N1 (Clontech), digested accordingly to produce pp7-GFP or pBVDVp7-GFP. All were verified by double-stranded DNA sequencing. The same PCR amplifier used to generate pCDNAp7 was cloned into pBluescript KS II+ (Stratagene) to make pKSp7. ssDNA was generated and the KR mutation introduced using a mutagenic oligonucleotide after the method of Kunkel *et al.* (1991), giving pKSp7KR. Constructs containing this mutation – pCDNAHIS₆p7KR, pCDNAFLAGp7KR, pp7KR-GFP – were generated using pKSp7KR as template in the same PCR methodology described above and verified by double-stranded DNA sequencing; All primer sequences are available on request.

Mammalian cell culture and transfection. Cells were maintained in Dulbecco's Modified Eagle's Medium (DMEM) supplemented with 10% fetal calf serum, 100 IU ml⁻¹ penicillin and 100 µg ml⁻¹ streptomycin. For Vero cell transfection, cells were grown to 40–70% confluency, infected with a recombinant fowlpox virus (FPV) expressing T7 RNA polymerase for 1 h, and then transfected using Lipofectamine (Invitrogen), according to the manufacturer's instructions, with 1 µg HA cDNA and 0.2 µg M2/p7 cDNA per well of a six-well plate. 293T cells were grown to 60–80% confluency either in wells of a six-well plate or on coverslips coated in poly(L-lysine) (Sigma) in a 12-well plate well and transfected using Lipofectamine with 2 or 1 µg DNA respectively. Co-transfections of GFP fusion plasmids and CFP marker constructs were made up of 0.5 µg of each plasmid.

Haemadsorption assay. This method is adapted from a published method (Takeuchi & Lamb, 1994; Medeiros *et al.*, 2001). Vero cells were infected and transfected as described above. 48 h post-transfection the cells were washed twice with PBS. 1 ml of 5.5 mU ml⁻¹ bacterial neuraminidase from *Vibrio cholerae* (Roche) diluted in serum-free DMEM was added to each well. The cells were incubated at 37 °C for 1 h and then washed three times to remove any traces of neuraminidase before addition of 1 ml of a 0.5% (w/v) suspension of horse red blood cells in PBS to each well. After incubation at room temperature for 2 h plates were gently shaken to resuspend unbound red blood cells and washed three times with PBS. Cells were lysed in 1 ml of CAT ELISA lysis buffer (Roche) for 3 min and the lysate was clarified in a microfuge at 13 000 r.p.m. for 5 min. Absorbance at 540 nm was recorded using a UV-2 UV/Vis spectrometer (Unicam).

Protein expression and immunoblotting. For detection of expressed proteins, transfected 293T or Vero cells from one well of a six-well plate were washed twice and scraped into 1 ml PBS. Cells were pelleted at 7000 r.p.m. for 2 min and lysed in 100 µl of EBC lysis buffer (50 mM Tris/HCl pH 8.0, 140 mM NaCl, 100 mM NaF, 200 µM Na₃VO₄, 0.1% SDS, 0.5% NP40). Following normalization of protein concentration using the BCA protein assay (Bio-Rad), 10 µl of lysate was subjected to SDS-PAGE and transferred to an Immobilon PVDF membrane (Millipore). FLAG tagged proteins were detected with an anti-FLAG M2 mouse monoclonal antibody

(Sigma) plus HRP–goat anti-mouse secondary (Sigma). BVDV p7 was detected using bovine hyperimmune anti-BVDV serum (donated by John McCauley, IAH, Compton, UK) plus HRP–rabbit anti-bovine secondary (Sigma). H5 HA was detected using a polyclonal sheep antiserum plus HRP–donkey anti-sheep secondary (Sigma).

Radiolabelled BVDV p7 and HIS₆-p7 were expressed *in vitro* using the TNT Quick coupled transcription/translation kit (Promega) with 1 µg of DNA and 10 µCi -Trans³⁵S-label (ICN), according to manufacturers' instructions. Following RNase A treatment, proteins were precipitated with 2 vols of acetone and resuspended in 20 µl Laemmli buffer; the sample was then split and subjected to SDS-PAGE. Gels were immunoblotted as described or fixed in 40% methanol/10% acetic acid, and then treated with Enlightning (NEN-Dupont) for 30 min prior to autoradiography.

Fluorescence analysis of FLAGp7 and GFP fusions. Cells to be labelled with MitoTracker red 580 nm (Molecular Probes) were incubated in a 200 nM solution of the dye in DMEM for 1 h prior to fixation. Cells transfected on coverslips were washed three times in PBS, fixed with 4% paraformaldehyde in PBS for 20 min at room temperature and then washed twice more in PBS. GFP/CFP-labelled cells were analysed at this point. Cells to be analysed by immunocytochemistry were permeabilized with 1% Triton X-100 in PBS or cold acetone (MitoTracker-labelled cells) for 5 min. Cells were washed three times and then incubated with FITC-conjugated mouse anti-FLAG monoclonal antibody (Sigma) diluted in 10% fetal calf serum/PBS for 1 h at room temperature in a dark humidified container. Nuclei were labelled with Hoechst stain (Molecular Probes) diluted 1/10 000 in PBS and the cells washed a further three times in PBS and then once in distilled water prior to analysis. Images were captured using a DeltaVision restoration system (Applied Precision Inc.), based around an Olympus IX-70 inverted microscope. Optical sections of 0.2 µm were captured with a CoolSNAP HQ CCD camera (Roper Scientific). Digital deconvolution and

image analysis were then performed on 3D datasets using 15 iterations of a constrained iterative deconvolution algorithm with SoftWoRx deconvolution software (Applied Precision Inc.).

RESULTS

HCV p7 contains a conserved basic loop

Fig. 1(a) shows an alignment of the p7 protein sequences from the currently available infectious molecular clones of HCV. The data typify over 500 p7 sequences analysed from different isolates (data not shown). All p7 sequences showed conservation of a short stretch of amino acids located between the two predicted *trans*-membrane alpha helices. This sequence, IKGR in genotype 1b, is rarely changed in other HCV isolates, and the K and R, at positions 33 and 35 respectively, are absolutely conserved by HCV except in a few cases where the two are exchanged. This suggests that the presence of charged residues at this locus is important for HCV p7 function. We previously used computer modelling to generate a predicted structure for a HCV p7 hexamer (Griffin *et al.*, 2003). In this model, the K and R side-chains of each monomer project into the lumen, constricting the aperture on the cytosolic side of the channel, suggesting that these residues form a gate to regulate the flow of ions. BVDV and other pestivirus p7 proteins possess a similar sequence containing charged residues. Mutation of this region in BVDV gave a similar phenotype to deleting the entire p7 open reading frame (ORF), abrogating virus infectivity in cell culture (Harada

A.

Amino acid	1	10	20	30	40	50	60
J4	AL	ENLVVLNNAAS	VAGAHGILSFLVFFCAAWY	IKGR LA	PGAAAYAFYGVWPL	LLLLLALPPRAYA	
H77		I	L T LV	F	WV	V L M	Q
N		A			V	A	T
Con1			I		V	L	
J6	K	I	A SCN F Y VI	V	VV	L T SLT L SFS	QQ
BVDV-1	VQYGAGEIVMMGNLLTHDSVEVVVTFLLLYLLL REENTKKWVI LIYHIIVMHPLKSVTVILLMVGGMKA						

B.

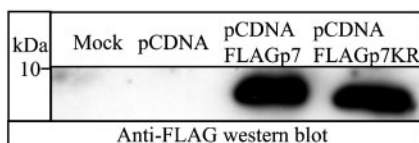


Fig. 1. Conservation of a basic loop domain in HCV p7. (A) Alignment of the p7 ORF from the full-length infectious clones of HCV genotypes 1 and 2. Variations from the J4 genotype 1b clone are listed and the conserved basic loop region is shown in bold. Predicted *trans*-membrane alpha helices are shaded. p7 from the BVDV-1 CP7 clone is also shown for comparison. (B) Western blot of 293T cell lysates expressing FLAG-tagged wild-type and KR mutant p7 with anti-FLAG monoclonal antibody. The same numbers of cells ($\sim 2 \times 10^5$) were transfected and lysed in each case and the protein concentration loaded was normalized by BCA assay (see Methods).

et al., 2000). To investigate the role of this region in HCV, we generated a mutation termed 'KR' in which K33 and R35 of the p7 sequence from the genotype 1b J4 infectious clone of HCV (Yanagi *et al.*, 1998) are changed to alanine residues. This mutation did not adversely affect the expression or stability of p7 compared to wild-type in 293T cells as assessed by Western blot using an N-terminally FLAG-tagged p7 protein (Fig. 1b). This was confirmed by later immunofluorescence studies (see Figs 4 and 5).

HCV p7 facilitates amantadine-sensitive transport of influenza virus H5 HA protein to the cell surface

To date, p7 ion channel function in mammalian cells has yet to be demonstrated and the nature of the ion specificity in cells is not known. Our finding that amantadine

specifically inhibits HCV p7 activity *in vitro* led us to investigate whether p7 function could be assessed in a system previously used to measure the activity of the influenza virus M2 ion channel (Ohuchi *et al.*, 1994; Takeuchi & Lamb, 1994). The system relies on the requirement for M2 to prevent protonation of exocytic vesicles carrying haemagglutinin (HA) protein with a multi-basic cleavage site to the cell surface (Ciampor *et al.*, 1992; Sakaguchi *et al.*, 1996). This multi-basic motif renders the precursor HA0 susceptible to cleavage by ubiquitous intracellular proteases such as furin, broadening virus tissue tropism. It also, however, places the newly synthesized HA at risk of a premature fusogenic conformational change at low pH. Consequently, transport of binding-competent multi-basic HA to the cell surface is M2 dependent and its binding to sialic acid on erythrocytes can be used as an indirect measure of M2 channel function (Fig. 2a).

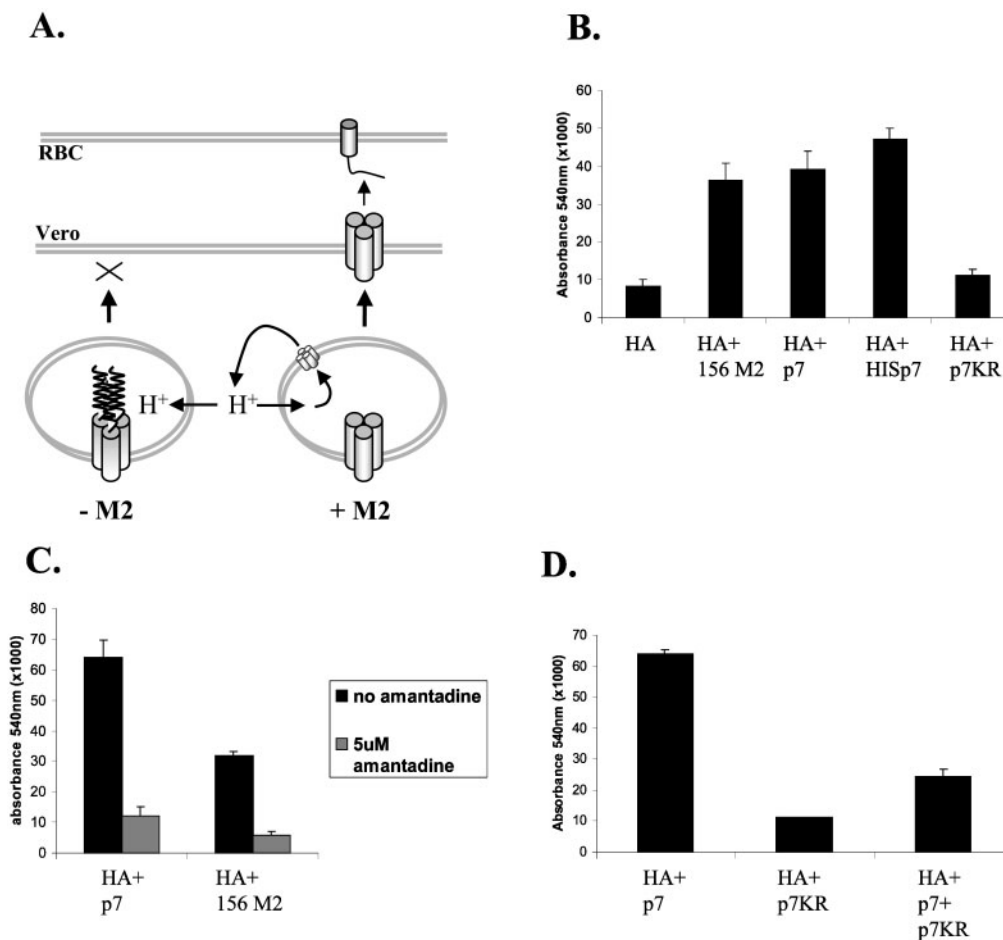


Fig. 2. HCV p7 facilitates transport of multibasic H5 HA to the cell surface. (A) Schematic diagram of haemadsorption assay showing maintenance of non-fusogenic H5 HA in the presence of M2 leading to its transport to the surface of transfected Vero cells and subsequent binding to sialic acid on the surface of erythrocytes. (B) Haemadsorption assay for Vero cells 48 h post-transfection with HA, HA and M2, HA and p7, HA and HIS₆-p7 or HA and HIS₆-p7KR. (C) Haemadsorption assay for Vero cells expressing HA with M2 or p7 in the presence/absence of 5 µM amantadine. (D) Haemadsorption of Vero cells expressing HA with HIS₆-p7, HIS₆-p7KR, or both. Error bars represent the SEM from at least two experiments in all cases.

Co-transfection of Vero cells with multi-basic H5 HA and p7 resulted in haemadsorption to levels comparable with those achieved with co-expression of H5 HA and M2, indicating that p7 was relieving the low pH of exocytic vesicles containing the HA protein (Fig. 2b). Addition of an epitope tag to the N terminus of p7 in the form of a six-histidine (HIS₆) tag was not detrimental to p7 function; indeed, the level of activity of this HIS₆-p7 protein was slightly higher than with the native protein or M2 (Fig. 2b). This is in accordance with our previous observation that a HIS₆-tagged p7 forms an effective ion channel in artificial membranes (Griffin *et al.*, 2003). Total levels of HA expression in parallel co-transfections of Vero cells were similar when M2, p7 or control vector was present (data not shown). Unfortunately, we were unable to detect p7 or HIS₆-p7 expressed in mammalian cells using a sheep anti-serum raised against bacterially expressed GST-HIS-p7 (Griffin *et al.*, 2003). It is likely, however, that the effects of having M2 and/or p7 present were not an artefact of overexpression as only one-fifth the amount of this DNA was used compared to the HA expression plasmid.

We previously showed that amantadine inhibited HCV p7 ion channel activity in artificial membranes (Griffin *et al.*, 2003) and it was of interest to determine the effect of the drug in a cell-based assay. Amantadine (5 μ M) reduced both M2- and p7-dependent haemadsorption to background levels observed when HA was transfected alone (Fig. 2c). As inhibition of M2 at this concentration in cell culture is known to be specific, it would appear that amantadine also specifically inhibits HCV p7 ion channel activity.

The HCV p7 basic loop is essential for ion channel activity

HCV HIS₆-p7 containing the KR mutation was assessed in the haemadsorption assay for ion channel activity. The mutation reduced the level of erythrocyte binding to baseline levels observed for HA alone (Fig. 2d). Furthermore, co-transfection (replacing half of the wild-type DNA with that of the mutant) of the KR mutant with wild-type p7 resulted in inhibition of the activity of the wild-type protein (Fig. 2d). This implied that both the KR and wild-type p7 were present in the same intracellular compartment and formed hetero-oligomers incapable of functioning as ion channels. The number of functional ion channels required for a positive read-out in this assay cannot be determined: it is possible, therefore, that the presence of a small number of functional channels amongst an excess of hetero-oligomers can yield a measurable effect. In contrast, mutations of residues in other parts of the protein (V13L, C27A and P49A; data not shown) resulted in only a slight reduction in activity in the assay.

BVDV p7 forms an oligomeric ion channel

The amino acid sequences of the p7 proteins from BVDV and HCV are relatively distant (Fig. 1a), yet they share a high degree of predicted structural homology. It was of

interest, therefore, to determine whether BVDV p7 could also function as an ion channel. A major feature of the viroporins is their ability to oligomerize in cellular membranes, as we have previously shown for HCV p7 (Griffin *et al.*, 2003). ³⁵S-labelled BVDV p7 and BVDV HIS₆-p7 were generated by *in vitro* translation in the presence of microsomal membranes and analysed by reducing SDS-PAGE. Both monomer and a higher molecular mass form, consistent with an oligomeric form of p7, were evident (Fig. 3a). Both the native p7 and the HIS-p7 oligomers were estimated to be pentameric by comparison with molecular mass standards. Interestingly, these complexes were extremely stable compared to HCV p7 oligomers, which required stabilization with chemical cross-linkers (Griffin *et al.*, 2003). Furthermore, immunoblotting the same *in vitro* translation reactions using bovine hyperimmune anti-BVDV serum detected only the oligomeric form, providing circumstantial

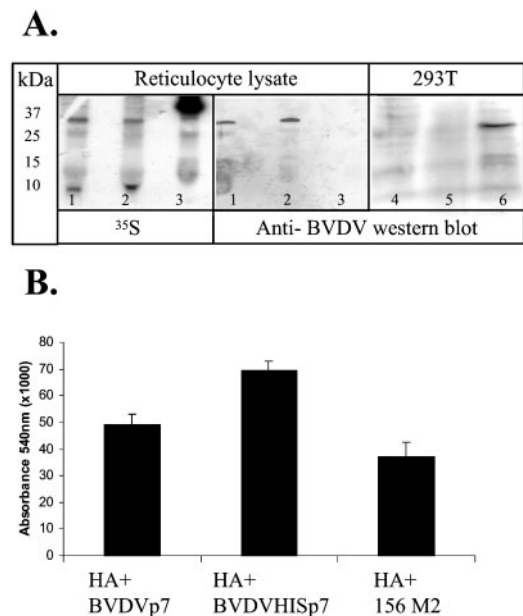


Fig. 3. BVDV p7 forms an oligomeric ion channel. (A) Left panel: ³⁵S-labelled BVDV p7 and HIS₆-p7 were generated *in vitro* by coupled transcription/translation reaction in rabbit reticulocyte lysates. Proteins were acetone-precipitated, subjected to SDS-PAGE on a 15% Tris/glycine gel, and visualized by autoradiography. Lanes: 1, BVDV p7; 2, BVDV HIS₆-p7; 3, luciferase control reaction. Middle panel: ³⁵S-labelled BVDV p7 and HIS₆-p7 were immunoblotted using hyperimmune bovine anti-BVDV serum and rabbit anti-bovine HRP-conjugated secondary antibody. Lanes as for left-hand panel. Right panel: protein was harvested from mock-, pCDNA- or pCDNABVDVp7-transfected 293T cells as described in Methods and immunoblotted as described for the middle panel. Lanes: 4, mock; 5, pCDNA; 6, pCDNABVDVp7. (B) Haemadsorption assay for HA with either M2, BVDV p7 or BVDV HIS₆-p7 in Vero cells. HA only control shown in Fig. 2 as experiments performed in parallel. Error bars represent the SEM from two or more separate experiments in all cases.

evidence that this is the predominant form in which BVDV p7 exists in natural infection. This form was also the only species detected when BVDV p7 was expressed in mammalian cells (Fig. 3a).

Given that BVDV p7 was capable of oligomerization, ion-channel activity was assessed using the haemadsorption assay. Both the native and HIS-p7 of BVDV displayed similar activity to HCV p7, confirming that the protein acts as an ion channel and that N-terminal epitope tags do not interfere with this function (figure 3b).

p7 partially localizes to an intracellular compartment associated with mitochondria

The negative effect on wild-type p7 function observed for the KR mutant implied that both it and the wild-type localize to the same intracellular compartment. Others have previously observed a reticular distribution of HCV p7 expressed in human HepG2 hepatoma cells, though the cellular compartment that this represented was not identified (Carrere-Kremer *et al.*, 2002). To analyse the subcellular distribution of p7 in more detail we generated expression constructs in which p7 was fused to eGFP at its C terminus and analysed its localization in transfected human 293T cells. These cells were found to express p7-GFP and other p7 derivatives most efficiently in a short time period, thereby avoiding cytotoxicity associated with long-term expression of these proteins. Similar fluorescence patterns were, however, observed in HepG2 and COS-7 cells transfected with these constructs (data not shown).

Surprisingly, expression of p7-GFP resulted in a punctate staining in the cytoplasm of transfected cells (Fig. 4b, c). This distribution was unaffected by the KR mutation and levels of expression appeared similar (Fig. 4d). To determine the nature of the cellular compartment that this punctate staining represented, cells were co-transfected with p7-GFP and cyan fluorescent protein (CFP)-tagged markers for Golgi, endoplasmic reticulum (ER) and mitochondria (Living Colours, Clontech). Neither the ER nor the Golgi CFP fluorescence co-localized with p7-GFP making it unlikely that the punctate staining pattern had arisen due to disruption of these organelles (Fig. 4e, f). The mitochondrial CFP marker, however, clearly overlapped with the signal from p7-GFP (Fig. 4g). Furthermore, expression of BVDV p7 fused to eGFP resulted in a fluorescence pattern similar to that seen with HCV p7-GFP, and this also overlapped with the signal from the mitochondrial marker (Fig. 4h).

It was important to ensure that the pattern of p7-GFP localization we observed was not an artefact of fusion to eGFP. We therefore expressed FLAG-p7 and stained permeabilized 293T cells with an FITC-conjugated monoclonal anti-FLAG antibody (Sigma) (Fig. 5a). Reassuringly, both FLAG-p7 and FLAG-p7KR displayed the same punctate form of staining as did the p7-GFP fusions (Fig. 5a, panels 1 and 2), though a second pattern of a more reticular appearance was also evident (Fig. 5a, panels 3 and 4). This pattern of staining was also observed when p7 with a C-terminal FLAG tag was expressed in the context of the other HCV structural proteins (Fig. 5c).

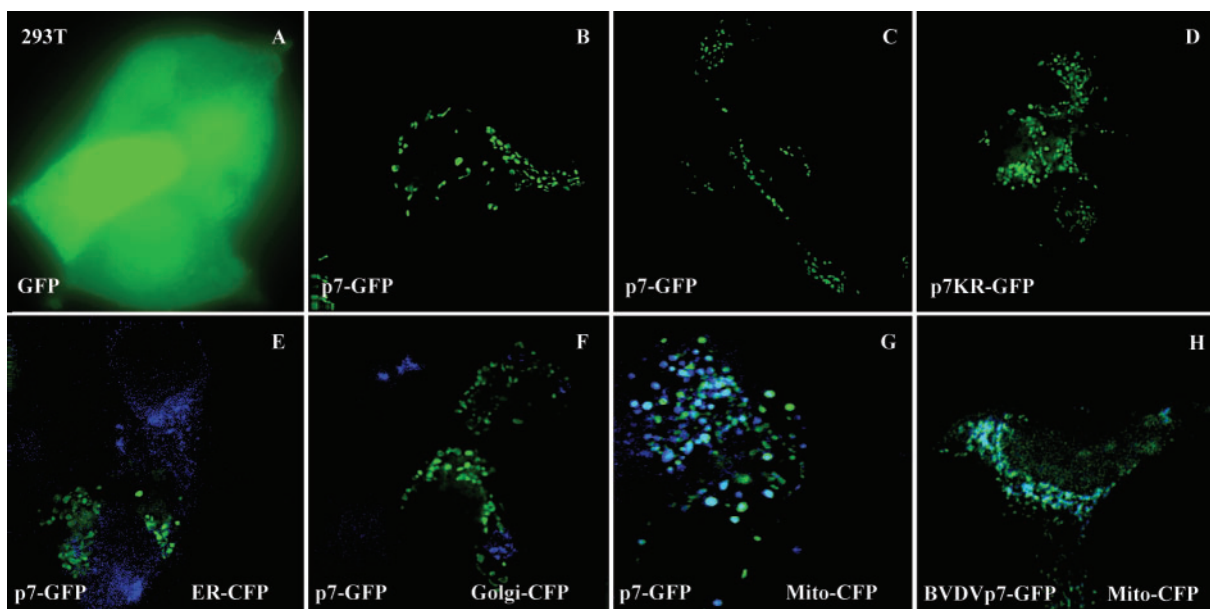


Fig. 4. p7-GFP fusion proteins localize to mitochondria in 293T cells. 293T cells grown on coverslips were transfected with plasmids pGFP-N1 (a), pp7-GFP (b, c), pp7KR-GFP (d), pp7-GFP with pER-CFP (e), pp7-GFP with pGolgi-CFP (f), pp7-GFP with pmitochondria-CFP (g) and pBVDVp7-GFP with pmitochondria-CFP (h). Shown are typical 0.2 μ m sections following digital deconvolution and overlay of images from FITC and CFP filters.

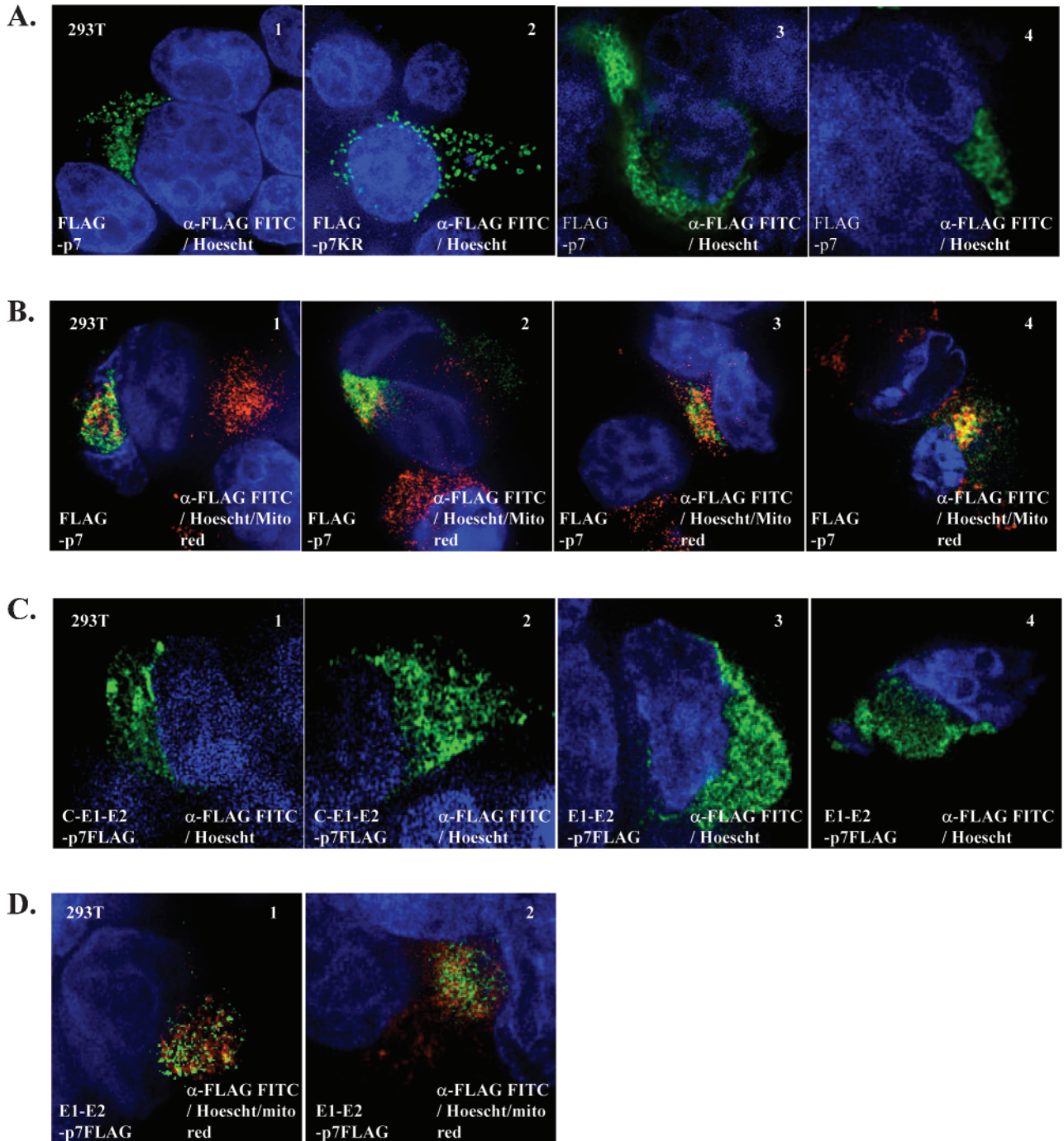


Fig. 5. Flag-p7 and FLAG-p7KR show punctate and reticular staining associated with mitochondria in 293T cells. 293T cells grown on coverslips were transfected with FLAG-tagged p7 proteins: either wild-type, with the KR mutation, or in the context of other HCV structural genes. In addition, parallel transfections were incubated with the MitoTracker red 580 nm specific dye as described in Methods. Shown are 0.2 μ m sections following digital deconvolution and overlay of FITC, Texas red and UV filters as appropriate. (A) Punctate and reticular staining of wild-type and KR mutant FLAG-p7 in 293T cells. (B) Co-localization of FLAG-p7 with MitoTracker red in 293T cells. (C) Reticular pattern of staining of p7-FLAG expressed in context of other HCV structural proteins: Core-E1-E2-p7FLAG (panels 1 and 2), E1-E2-p7FLAG (panels 3 and 4). (D) Co-localization of p7 with MitoTracker red expressed in context of E1-E2-p7FLAG.

To determine whether the reticular pattern of staining was also due to association with mitochondria, 293T cells expressing FLAG-p7 or p7-FLAG in the context of other HCV structural proteins were incubated with a mitochondrion-specific dye, MitoTracker red 580 nm (Molecular Probes). This dye specifically accumulates in the membranes of mitochondria in live cells and remains stable post-fixation. In all cases a significant overlap of the anti-FLAG FITC and MitoTracker signal was observed in cells positive for p7 expression, though regions positive for one or the other dye were also evident (Fig. 5b, d). This suggests that p7 was present not only in a mitochondrion-associated compartment, but also in adjacent membrane structures (Fig. 5b, d).

DISCUSSION

We have shown that p7 proteins of HCV and BVDV act as ion channels in the membranes of mammalian cells. Both were active in an assay necessitating the disruption of proton gradients in exocytic vesicles carrying influenza virus HA to the surface of transfected Vero cells. The ion specificity of p7, however, is not yet known and it is not possible to infer that it forms a proton channel based on these observations. A recent report, however, found HCV E1 and E2 to be pH-sensitive: low pH rendered them incapable of permitting the entry of pseudotyped retroviral particles (Hsu *et al.*, 2003). Given the activity of p7 in the haemadsorption assay, it is tempting to speculate that one of its functions may be to protect E1 and E2 from pH changes during the egress of HCV particles from infected cells. We are currently undertaking measurement of p7 channel permeability by single-cell patch clamp to determine its ion specificity.

Amantadine abrogated the activity of p7 in the haemadsorption assay at concentrations known to specifically inhibit M2 in cell culture. This is consistent with our finding that the drug also inhibited channel formation in artificial membranes at similar concentrations (Griffin *et al.*, 2003). Amantadine inhibits M2 by preventing the protonation of a histidine residue and its subsequent interaction with a tryptophan residue in the channel lumen, thus preventing channel opening (Duff *et al.*, 1994; Wang *et al.*, 1995; Salom *et al.*, 2000; Okada *et al.*, 2001). Interestingly, a conserved histidine residue is also present at position 17 in both HCV and BVDV p7 located within the N-terminal predicted *trans*-membrane alpha helix, though its role in ion channel function has yet to be determined. Amantadine has been used in clinical trials alongside current regimes with some success (Brillanti *et al.*, 2000; Cozzolongo *et al.*, 2002; Zilly *et al.*, 2002; Berg *et al.*, 2003; Piai *et al.*, 2003; Thuluvath *et al.*, 2003; Weegink *et al.*, 2003). The mode of action of amantadine in these cases is unclear, though we propose that it acts by inhibiting p7 ion channel function (Martin *et al.*, 1999; Jubin *et al.*, 2000; Griffin *et al.*, 2003).

The high degree of conservation in the basic loop region of

HCV p7 suggests its importance for function and this was demonstrated by our finding that the KR mutant protein had lost ion channel activity. Our previous model of a p7 oligomeric channel predicted that the side-chains from K and R project into the channel lumen, perhaps forming a gate controlling the flow of ions (Griffin *et al.*, 2003). Mutation of the analogous region in BVDV has previously been shown to abrogate virus infectivity in culture (Harada *et al.*, 2000). It is unlikely that the KR mutation caused decreased stability of the ion channel complex as co-expression with the wild-type protein resulted in a negative effect on wild-type function. The most plausible explanation for this is that the two proteins were present in the same intracellular compartment and were able to hetero-oligomerize forming a non-functional channel. In addition, it is likely that residues present in the *trans*-membrane alpha helices are responsible for the stable formation of oligomers, as has been suggested previously (Carrere-Kremer *et al.*, 2002).

During the preparation of this manuscript, it was shown that both deletion of p7 and mutating the KR loop abrogated replication of genotype 1a infectious RNA in chimpanzees (Sakai *et al.*, 2003). Our demonstration that the KR loop is essential for genotype 1b p7 ion channel function makes it likely that this phenotype arose due to a similar defect in this activity for the 1a genotype. Furthermore, chimeras in which the 1a sequence was replaced with the 2a genotype were non-functional except in one case where the termini of the protein remained the parental genotype. This implied that p7 might interact with other viral gene products in a genotype-dependent fashion via these termini. Nevertheless, the demonstration that the 2a *trans*-membrane domains and KR loop could replace that of 1a supports the suggestion that p7 acts as an ion channel in all HCV genotypes.

The localization of p7 was unaffected by the KR mutation in transfected 293T cells. p7-GFP showed a punctate staining pattern, quite dissimilar to that shown in previous investigations of p7 cellular distribution (Carrere-Kremer *et al.*, 2002) and this corresponded to at least partial localization to mitochondria. Expression of FLAG-p7 also gave a similar pattern in cells, though other more reticular staining was also apparent which significantly co-localized with mitochondria visualized with a specific stain. This pattern was also observed when p7 was expressed in the context of the other HCV structural proteins. Previously, p7 has been shown to display a reticular staining pattern in HepG2 cells leading to the supposition that the protein is mainly present in the ER, though no markers for cellular organelles were used to confirm this (Carrere-Kremer *et al.*, 2002). Interestingly, other HCV gene products have been shown to localize to membrane cisternae closely associated with mitochondria in replicon-bearing cells (Mottola *et al.*, 2002). An explanation for these different staining patterns could be that in dividing cells the morphology of mitochondria is known to vary between a classical punctate ovoid

shape, with which they are usually associated, and a reticulum where the organelle is a continuous entity.

Recently, it has become apparent that a number of virally expressed proteins have the ability to localize to mitochondria and affect apoptotic pathways via alteration of mitochondrial membrane permeability: e.g. human immunodeficiency virus (HIV) Vpr (Jacotot *et al.*, 2001), human T-cell lymphotropic virus (HTLV-1) p13^{II} (D'Agostino *et al.*, 2002), hepatitis B virus (HBV) X protein (Takada *et al.*, 1999; Rahmani *et al.*, 2000) and influenza virus PB1 ORF 2 (Gibbs *et al.*, 2003). These are targeted to mitochondria via mechanisms differing from that of most cellular proteins, which possess canonical N-terminal targeting sequences. Instead, targeting signals are contained within the protein itself and are not proteolytically cleaved. The insertion of these proteins into mitochondrial membranes is thought to occur via a similar mechanism to that used by the cellular voltage-dependent anion channel (VDAC), the adenine nucleotide translocator (ANT) and Bcl-2 family proteins. These are major regulators of mitochondrial permeability (Halestrap & Brennerb, 2003) and are known to interact with several of these viral proteins (Boya *et al.*, 2001, 2003). It is likely that both HCV and BVDV p7 are targeted to mitochondrial membranes in a similar fashion, suggesting they may modulate apoptosis. This does not preclude that p7 possess other functions when present in other cellular compartments, as suggested by the observed incomplete overlap with mitochondrial markers. This is also the case for many other viroporins including HIV-1 Vpr, which is known to affect apoptosis when present in mitochondria yet plays several other roles in the virus life-cycle (Piller *et al.*, 1996, 1999; Lamb & Pinto, 1997; Halestrap & Brennerb, 2003). For example, some data are suggestive of a role for p7 in the entry of HCV virus-like particles (Saunier *et al.*, 2003). Currently, the precise role of p7 in the HCV life-cycle is difficult to determine; however, given the importance of other viroporins for virus replication, the specific inhibition of HCV p7 by amantadine represents an opportunity for a new direction of research for antiviral chemotherapy.

ACKNOWLEDGEMENTS

We thank Gareth Howell for support and advice on fluorescence microscopy, Jeus Bukh for HCV and Gregor Meyers for BVDV clones, Mike Skinner for the recombinant fowlpox and Matthew Bentham for useful discussion. This work was funded by the MRC (grant no. G0 000321). R. H. was in receipt of a grant from PHLS.

REFERENCES

Aldabe, R. & Carrasco, L. (1995). Induction of membrane proliferation by poliovirus proteins 2C and 2BC. *Biochem Biophys Res Commun* **206**, 64–76.

Berg, T., Kronenberger, B., Hinrichsen, H. & 10 other authors (2003). Triple therapy with amantadine in treatment-naïve patients with chronic hepatitis C: a placebo-controlled trial. *Hepatology* **37**, 1359–1367.

Boya, P., Roques, B. & Kroemer, G. (2001). New EMBO members' review: viral and bacterial proteins regulating apoptosis at the mitochondrial level. *EMBO J* **20**, 4325–4331.

Boya, P., Roumier, T., Andreau, K., Gonzalez-Polo, R. A., Zamzami, N., Castedo, M. & Kroemer, G. (2003). Mitochondrion-targeted apoptosis regulators of viral origin. *Biochem Biophys Res Commun* **304**, 575–581.

Brillanti, S., Levantesi, F., Masi, L., Foli, M. & Bolondi, L. (2000). Triple antiviral therapy as a new option for patients with interferon nonresponsive chronic hepatitis C. *Hepatology* **32**, 630–634.

Carrere-Kremer, S., Montpellier-Pala, C., Cocquereel, L., Wychowski, C., Penin, F. & Dubuisson, J. (2002). Subcellular localization and topology of the p7 polypeptide of hepatitis C virus. *J Virol* **76**, 3720–3730.

Choo, Q. L., Kuo, G., Weiner, A., Wang, K. S., Overby, L., Bradley, D. & Houghton, M. (1992). Identification of the major, parenteral non-A, non-B hepatitis agent (hepatitis C virus) using a recombinant cDNA approach. *Semin Liver Dis* **12**, 279–288.

Ciampor, F., Bayley, P. M., Nermut, M. V., Hirst, E. M., Sugrue, R. J. & Hay, A. J. (1992). Evidence that the amantadine-induced, M2-mediated conversion of influenza A virus hemagglutinin to the low pH conformation occurs in an acidic trans Golgi compartment. *Virology* **188**, 14–24.

Clarke, B. (1997). Molecular virology of hepatitis C virus. *J Gen Virol* **78**, 2397–2410.

Cozzolongo, R., Cuppone, R. & Manghisi, O. G. (2002). The treatment of chronic hepatitis C not responding to interferon. *Curr Pharm Des* **8**, 967–975.

D'Agostino, D. M., Ranzato, L., Arrigoni, G. & 10 other authors (2002). Mitochondrial alterations induced by the p13II protein of human T-cell leukemia virus type 1. Critical role of arginine residues. *J Biol Chem* **277**, 34424–34433.

Duff, K. C. & Ashley, R. H. (1992). The transmembrane domain of influenza A M2 protein forms amantadine-sensitive proton channels in planar lipid bilayers. *Virology* **190**, 485–489.

Duff, K. C., Gilchrist, P. J., Saxena, A. M. & Bradshaw, J. P. (1994). Neutron diffraction reveals the site of amantadine blockade in the influenza A M2 ion channel. *Virology* **202**, 287–293.

Egger, D., Wolk, B., Gosert, R., Bianchi, L., Blum, H. E., Moradpour, D. & Bienz, K. (2002). Expression of hepatitis C virus proteins induces distinct membrane alterations including a candidate viral replication complex. *J Virol* **76**, 5974–5984.

Ewart, G. D., Sutherland, T., Gage, P. W. & Cox, G. B. (1996). The Vpu protein of human immunodeficiency virus type 1 forms cation-selective ion channels. *J Virol* **70**, 7108–7115.

Gibbs, J. S., Malide, D., Hornung, F., Bennink, J. R. & Yewdell, J. W. (2003). The influenza A virus PB1-F2 protein targets the inner mitochondrial membrane via a predicted basic amphipathic helix that disrupts mitochondrial function. *J Virol* **77**, 7214–7224.

Gonzalez, M. E. & Carrasco, L. (1998). The human immunodeficiency virus type 1 Vpu protein enhances membrane permeability. *Biochemistry* **37**, 13710–13719.

Griffin, S. D., Beales, L. P., Clarke, D. S., Worsfold, O., Evans, S. D., Jaeger, J., Harris, M. P. & Rowlands, D. J. (2003). The p7 protein of hepatitis C virus forms an ion channel that is blocked by the antiviral drug, Amantadine. *FEBS Lett* **535**, 34–38.

Halestrap, A. P. & Brennerb, C. (2003). The adenine nucleotide translocase: a central component of the mitochondrial permeability transition pore and key player in cell death. *Curr Med Chem* **10**, 1507–1525.

- Harada, T., Tautz, N. & Thiel, H. J. (2000). E2-p7 region of the bovine viral diarrhoea virus polyprotein: processing and functional studies. *J Virol* **74**, 9498–9506.
- Hay, A. J., Wolstenholme, A. J., Skehel, J. J. & Smith, M. H. (1985). The molecular basis of the specific anti-influenza action of amantadine. *EMBO J* **4**, 3021–3024.
- Hsu, M., Zhang, J., Flint, M., Logvinoff, C., Cheng-Mayer, C., Rice, C. M. & McKeating, J. A. (2003). Hepatitis C virus glycoproteins mediate pH-dependent cell entry of pseudotyped retroviral particles. *Proc Natl Acad Sci U S A* **100**, 7271–7276.
- Jacotot, E., Ferri, K. F., El Hamel, C. & 17 other authors (2001). Control of mitochondrial membrane permeabilization by adenine nucleotide translocator interacting with HIV-1 viral protein rR and Bcl-2. *J Exp Med* **193**, 509–519.
- Jubin, R., Murray, M. G., Howe, A. Y., Butkiewicz, N., Hong, Z. & Lau, J. Y. (2000). Amantadine and rimantadine have no direct inhibitory effects against hepatitis C viral protease, helicase, ATPase, polymerase, and internal ribosomal entry site-mediated translation. *J Infect Dis* **181**, 331–334.
- Kunkel, T. A., Bebenek, K. & McClary, J. (1991). Efficient site-directed mutagenesis using uracil-containing DNA. *Methods Enzymol* **204**, 125–139.
- Lamb, R. A. & Pinto, L. H. (1997). Do Vpu and Vpr of human immunodeficiency virus type 1 and NB of influenza B virus have ion channel activities in the viral life cycles? *Virology* **229**, 1–11.
- Liljestrom, P., Lusa, S., Huylebroeck, D. & Garoff, H. (1991). In vitro mutagenesis of a full-length cDNA clone of Semliki Forest virus: the small 6,000-molecular-weight membrane protein modulates virus release. *J Virol* **65**, 4107–4113.
- Lin, C., Lindenbach, B. D., Pragai, B. M., McCourt, D. W. & Rice, C. M. (1994). Processing in the hepatitis C virus E2-NS2 region: identification of p7 and two distinct E2-specific products with different C termini. *J Virol* **68**, 5063–5073.
- Loewy, A., Smyth, J., von Bonsdorff, C. H., Liljestrom, P. & Schlesinger, M. J. (1995). The 6-kilodalton membrane protein of Semliki Forest virus is involved in the budding process. *J Virol* **69**, 469–475.
- Martin, J., Navas, S., Fernandez, M., Rico, M., Pardo, M., Quiroga, J. A., Zahm, F. & Carreno, V. (1999). In vitro effect of amantadine and interferon alpha-2a on hepatitis C virus markers in cultured peripheral blood mononuclear cells from hepatitis C virus-infected patients. *Antivir Res* **42**, 59–70.
- Medeiros, R., Escriou, N., Naffakh, N., Manuguerra, J. C. & van der Werf, S. (2001). Hemagglutinin residues of recent human A(H3N2) influenza viruses that contribute to the inability to agglutinate chicken erythrocytes. *Virology* **289**, 74–85.
- Meyers, G., Tautz, N., Becher, P., Thiel, H. J. & Kummerer, B. M. (1996). Recovery of cytopathogenic and noncytopathogenic bovine viral diarrhoea viruses from cDNA constructs. *J Virol* **70**, 8606–8613.
- Mizushima, H., Hijikata, M., Asabe, S., Hirota, M., Kimura, K. & Shimotohno, K. (1994). Two hepatitis C virus glycoprotein E2 products with different C termini. *J Virol* **68**, 6215–6222.
- Mottola, G., Cardinali, G., Ceccacci, A., Trozzi, C., Bartholomew, L., Torrisi, M. R., Pedrazzini, E., Bonatti, S. & Migliaccio, G. (2002). Hepatitis C virus nonstructural proteins are localized in a modified endoplasmic reticulum of cells expressing viral subgenomic replicons. *Virology* **293**, 31–43.
- Newton, K., Meyer, J. C., Bellamy, A. R. & Taylor, J. A. (1997). Rotavirus nonstructural glycoprotein NSP4 alters plasma membrane permeability in mammalian cells. *J Virol* **71**, 9458–9465.
- Ohuchi, M., Cramer, A., Vey, M., Ohuchi, R., Garten, W. & Klenk, H. D. (1994). Rescue of vector-expressed fowl plague virus hemagglutinin in biologically active form by acidotropic agents and coexpressed M2 protein. *J Virol* **68**, 920–926.
- Okada, A., Miura, T. & Takeuchi, H. (2001). Protonation of histidine and histidine-tryptophan interaction in the activation of the M2 ion channel from influenza A virus. *Biochemistry* **40**, 6053–6060.
- Pavlovic, D., Neville, D. C., Argaud, O., Blumberg, B., Dwek, R. A., Fischer, W. B. & Zitzmann, N. (2003). The hepatitis C virus p7 protein forms an ion channel that is inhibited by long-alkyl-chain iminosugar derivatives. *Proc Natl Acad Sci U S A* **100**, 6104–6108.
- Piai, G., Rocco, P., Tartaglione, M. T. & 7 other authors (2003). Triple (interferon, ribavirin, amantadine) versus double (interferon, ribavirin) re-therapy for interferon relapsing genotype 1b HCV chronic active hepatitis patients. *Hepatol Res* **25**, 355–363.
- Piller, S. C., Ewart, G. D., Premkumar, A., Cox, G. B. & Gage, P. W. (1996). Vpr protein of human immunodeficiency virus type 1 forms cation-selective channels in planar lipid bilayers. *Proc Natl Acad Sci U S A* **93**, 111–115.
- Piller, S. C., Ewart, G. D., Jans, D. A., Gage, P. W. & Cox, G. B. (1999). The amino-terminal region of Vpr from human immunodeficiency virus type 1 forms ion channels and kills neurons. *J Virol* **73**, 4230–4238.
- Pinto, L. H., Holsinger, L. J. & Lamb, R. A. (1992). Influenza virus M2 protein has ion channel activity. *Cell* **69**, 517–528.
- Rahmani, Z., Huh, K. W., Lasher, R. & Siddiqui, A. (2000). Hepatitis B virus X protein colocalizes to mitochondria with a human voltage-dependent anion channel, HVDAC3, and alters its transmembrane potential. *J Virol* **74**, 2840–2846.
- Robertson, B., Myers, G., Howard, C. & 14 other authors (1998). Classification, nomenclature, and database development for hepatitis C virus (HCV) and related viruses: proposals for standardization. International Committee on Virus Taxonomy. *Arch Virol* **143**, 2493–2503.
- Sakaguchi, T., Leser, G. P. & Lamb, R. A. (1996). The ion channel activity of the influenza virus M2 protein affects transport through the Golgi apparatus. *J Cell Biol* **133**, 733–747.
- Sakai, A., Claire, M. S., Faulk, K., Govindarajan, S., Emerson, S. U., Purcell, R. H. & Bukh, J. (2003). The p7 polypeptide of hepatitis C virus is critical for infectivity and contains functionally important genotype-specific sequences. *Proc Natl Acad Sci U S A* **100**, 11646–11651.
- Salom, D., Hill, B. R., Lear, J. D. & DeGrado, W. F. (2000). pH-dependent tetramerization and amantadine binding of the transmembrane helix of M2 from the influenza A virus. *Biochemistry* **39**, 14160–14170.
- Saunier, B., Triyatni, M., Ulianich, L., Maruvada, P., Yen, P. & Kohn, L. D. (2003). Role of the asialoglycoprotein receptor in binding and entry of hepatitis C virus structural proteins in cultured human hepatocytes. *J Virol* **77**, 546–559.
- Schmidt-Mende, J., Bieck, E., Hugle, T., Penin, F., Rice, C. M., Blum, H. E. & Moradpour, D. (2001). Determinants for membrane association of the hepatitis C virus RNA-dependent RNA polymerase. *J Biol Chem* **276**, 44052–44063.
- Takada, S., Shirakata, Y., Kaneniwa, N. & Koike, K. (1999). Association of hepatitis B virus X protein with mitochondria causes mitochondrial aggregation at the nuclear periphery, leading to cell death. *Oncogene* **18**, 6965–6973.
- Takeuchi, K. & Lamb, R. A. (1994). Influenza virus M2 protein ion channel activity stabilizes the native form of fowl plague virus hemagglutinin during intracellular transport. *J Virol* **68**, 911–919.
- Thuluvath, P. J., Pande, H. & Maygers, J. (2003). Combination therapy with interferon-alpha(2b), ribavirin, and amantadine in

chronic hepatitis C nonresponders to interferon and ribavirin. *Dig Dis Sci* **48**, 594–597.

Tian, P., Estes, M. K., Hu, Y., Ball, J. M., Zeng, C. Q. & Schilling, W. P. (1995). The rotavirus nonstructural glycoprotein NSP4 mobilizes Ca^{2+} from the endoplasmic reticulum. *J Virol* **69**, 5763–5772.

van Kuppeveld, F. J., Hoenderop, J. G., Smeets, R. L., Willems, P. H., Dijkman, H. B., Galama, J. M. & Melchers, W. J. (1997). Coxsackievirus protein 2B modifies endoplasmic reticulum membrane and plasma membrane permeability and facilitates virus release. *EMBO J* **16**, 3519–3532.

Wang, C., Lamb, R. A. & Pinto, L. H. (1995). Activation of the M2 ion channel of influenza virus: a role for the transmembrane domain histidine residue. *Biophys J* **69**, 1363–1371.

Weegink, C. J., Sentjens, R. E., Beld, M. G., Dijkgraaf, M. G. & Reesink, H. W. (2003). Chronic hepatitis C patients with a post-treatment virological relapse re-treated with an induction dose of 18 MU interferon-alpha in combination with ribavirin and amantadine: a two-arm randomized pilot study. *J Viral Hepat* **10**, 174–182.

Yanagi, M., St Claire, M., Shapiro, M., Emerson, S. U., Purcell, R. H. & Bukh, J. (1998). Transcripts of a chimeric cDNA clone of hepatitis C virus genotype 1b are infectious in vivo. *Virology* **244**, 161–172.

Zilly, M., Lingenauber, C., Desch, S., Vath, T., Klinker, H. & Langmann, P. (2002). Triple antiviral re-therapy for chronic hepatitis C with interferon-alpha, ribavirin and amantadine in nonresponders to interferon-alpha and ribavirin. *Eur J Med Res* **7**, 149–154.